IEEE Access
Multidisciplinary | Rapid Review | Open Access Journal

Received June 6, 2021, accepted June 17, 2021, date of publication June 25, 2021, date of current version July 2, 2021.

Digital Object Identifier 10.1109/ACCESS.2021.3091735

Study on the Influence of Reignition on Electrical Life Distribution of Low-Voltage Circuit Breakers

ZHENGJUN LIU[1], (Graduate Student Member, IEEE), SHAOPO HUANG[1], AND CHENGCHEN ZHAO[2]

[1]State Key Laboratory of Reliability and Intelligence of Electrical Equipment, Hebei University of Technology, Tianjin 300130, China
[2]Key Laboratory of Electromagnetic Field and Electrical Apparatus Reliability of Hebei Province, Hebei University of Technology, Tianjin 300130, China

Corresponding author: Zhengjun Liu (liuzhengjun8000@163.com)

This work was supported in part by the National Natural Science Foundation of China under Grant 51777056, in part by the Graduate Student Innovation Ability Cultivation Funding Foundation of Hebei Province under Grant CXZZBS2018039, and in part by the Scientific Research Project of Tianjin Municipal Education Commission under Grant 2020KJ093.

ABSTRACT This study analyzes the recovery voltage changes when a low-voltage circuit breaker opens with load and short-circuit faults and explains the reignition types under different recovery voltages. Reignition probability models of a single-pole contact and three-pole contact under different reignition types are established. The variation law of the contact erosion amount with the arc starting phase angle is analyzed. The distribution characteristics of the electrical life under three reignition types are obtained by simulating the low-voltage circuit breaker electrical life with a random arc starting phase angle. The results show that the electrical life of contacts obviously decreases after reignition, and that the electrical life changes differently with different reignition types. Specifically, the electrical life of a single-pole contact and three-pole contact is reduced by different degrees for the same reignition type. Hence, the influence of reignition on the electrical life distribution characteristics of a low-voltage circuit breaker cannot be ignored.

INDEX TERMS Electrical life distribution, low-voltage circuit breaker, recovery voltage, reignition probability model.

I. INTRODUCTION

Low-voltage circuit breakers are a protective electrical appliance widely used in low-voltage distributions. It can turn on, bear, break rated current under normal running conditions, and bear and break the overloaded current within a stipulated time. The electrical life index of a low-voltage circuit breaker is related to the reliability and stability of distributed power lines. The study of the electrical life distribution of a low-voltage circuit breaker is the foundation of the power distribution reliability evaluation. Low-voltage circuit breakers are widely used in power distributions. For the analysis of its running state and performance, a clear understanding and judgment of the low-voltage circuit breakers' life distribution is needed [1]–[3].

The electrical life of a low-voltage circuit breaker mainly depends on arc erosion during interruption. When arc erosion reaches a certain extent, the electric contact state and arc extinguishing reliability are affected [4]–[6]. The switch apparatus electrical life calculation methods include the accumulative arc energy method, relative electric wear method, and weighting breaking current accumulation method [7], [8].

The performance degradation and state evaluation of low-voltage circuit breaker contacts are also an essential part of electrical life research. In [9], the normal distribution variable is constructed by the erosion loss segmenting accumulation. The Wiener process is used to predict the contact performance degradation curve of low-voltage electrical appliances. In addition, the contact resistance method is proposed. Some scholars take contact resistance as the research object, establish the electrical contact failure model, and judge the contacts' electrical performance through contact resistance [10], [11]. In research on the state evaluation of the circuit breaker electrical life, with intelligent sensors and monitoring equipment, the circuit breaker running state is quantitatively evaluated by analyzing its on-site monitoring signals [12]. Then, we can perform fault analysis and maintenance priority based on a time series to monitor the running status of low-voltage circuit breakers in real time. In [13], an online test for arc energy is proposed. It can measure the

The associate editor coordinating the review of this manuscript and approving it for publication was Ton Duc Do.

arc voltage and transient recovery voltage accurately, and the arc current is obtained through a current transformer. Finally, the contact life of the circuit breaker is evaluated using arc energy.

In contact erosion, the Mayr model of arc plasma between contacts is proposed under AC conditions [14]. The arc parameters are estimated by nonlinear curve fitting, and the correspondence between each parameter and the arc is analyzed, which can describe the arcing more accurately. In [15], an air arcing simulation model of the low-voltage circuit breaker is established using the ANSYS CFX software. The influence of the current and arc starting point on the arc movement of the low-voltage circuit breaker is analyzed. The model is verified by high-speed cameras. In [16], some arc erosion characteristic parameters of the contact surface are explored, such as macromorphology, micromorphology, and microstructure, with a 3-D profiler and scanning electron microscope. The arc formation and erosion mechanism of the Ag/CdO contact material are discussed.

Reliability research on low-voltage circuit breakers mainly focuses on arc erosion and contact performance degradation. However, in low-voltage power distribution, people are further concerned about the life distribution of low-voltage circuit breakers because it relates to the running and maintenance policy adjustment. It is also aimed at the overall understanding of the distribution line reliability. During the interruption, there is an arc between low-voltage circuit breaker contacts, which causes contact wear because of arc erosion [17], [18]. The arcing time and arc current are the major factors of arc erosion. In traditional research on the electrical life of a low-voltage circuit breaker, it is considered that the arc is extinguished at the AC current zero-crossing. The electrical life distribution characteristics are then analyzed by the accumulative arc energy method [13], [19]. Due to the existence of overvoltage, there is a certain probability that the arc reignites. Many scholars have studied the arc characteristics and reignition mechanism of circuit breakers [20]–[22]. However, the relationship between arc reignition and the electrical life distribution characteristics of low-voltage circuit breakers has been neglected. Before low-voltage circuit breakers leave the factory, the manufacturer carries out the life test on them. Nevertheless, it is limited to testing under a single load condition. The arc reignition situation changes with load conditions and line parameters. Then, the arc erosion on contacts increases. At this time, we need to reassess the low-voltage circuit breaker electrical life [23], [24]. Therefore, it is necessary to establish the reignition probability model of a low-voltage circuit breaker and analyze the electrical life distribution characteristics considering the reignition.

This paper starts from the elementary solution of a linear circuit and analyzes the reignition types under different recovery voltages with the help of the hypothesis of breakdown probability. Then, we establish the reignition probability model and introduce the concept of the minimum reignition phase angle. It can help to judge electrical life distribution more accurately under different grid parameters. Simultaneously, we analyze the variation law of contact erosion with arc starting phase angle (ASPA) when reignition occurs. We obtain the electrical life distribution characteristics of single-pole and three-pole contacts under different working conditions by Monte Carlo simulation. The results show that, compared with the traditional method, the arc erosion model considering reignition improves the accuracy of life assessment under different loads and running conditions. The research results provide theoretical support for reliability assessment and maintenance policy adjustment of the low-voltage circuit breaker.

II. REIGNITION PROBABILITY MODEL OF THE LOW-VOLTAGE CIRCUIT BREAKER

The primary condition for gap breakdown and arc reignition of the low-voltage circuit breaker is that the voltage between contacts reaches the critical voltage. The electron density in the contact gap (refers to the distance between contacts at the current zero-crossing) reaches a specific value to meet the discharge conditions. Therefore, the low-voltage circuit breaker reignition is related to the recovery voltage, gap distance, and dielectric state between contacts.

The ASPA of the low-voltage circuit breaker is random during the interruption, and the size of the contact gap (when the current crosses zero) varies with the ASPA. We can describe the reignition probability of a low-voltage circuit breaker under different running conditions by analyzing the recovery voltage waveform. Furthermore, the arc erosion laws under different reignition probabilities are analyzed, and the influence of reignition on the electrical life distribution characteristics of low-voltage circuit breakers is obtained. The amplitude and waveform of the recovery voltage are different under different load and line parameters, breaking with load or short-circuit faults.

A. RECOVERY VOLTAGE WAVEFORM OF LOW-VOLTAGE CIRCUIT BREAKER

The equivalent circuit diagram of a typical low-voltage circuit breaker breaking load circuit is shown in Fig. 1. R_1, L_1, C_1 are the equivalent resistance, inductance, and capacitance, respectively, on the power supply side, and on the load side, R_2, L_2, and C_2.

The load circuit is disconnected, and the voltages at both ends of C_1 and C_2 are u_{C1} and u_{C2}. The recovery voltage at both ends of the low-voltage circuit breaker contacts is described as $u_r = u_{C1} - u_{C2}$. When a short-circuit fault occurs on the load side (C_2, L_2, R_2), the circuit breaker recovery voltage is equal to the voltage of C_1, that is, $u_r = u_{C1}$.

The recovery voltage is composed of two parts: the power frequency component and the transient component. According to the different R_2, L_2, and C_2, there are two kinds of recovery voltage waveforms: an exponential waveform and an oscillating waveform. Fig. 2 is a schematic diagram of the recovery voltage waveform of the low-voltage circuit.

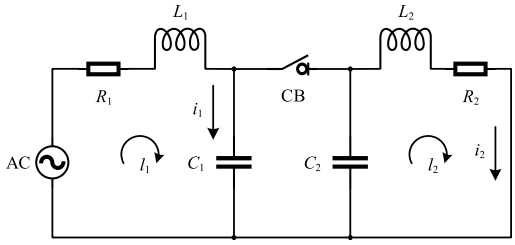

FIGURE 1. Equivalent circuit of the low-voltage circuit breaker breaking load circuit.

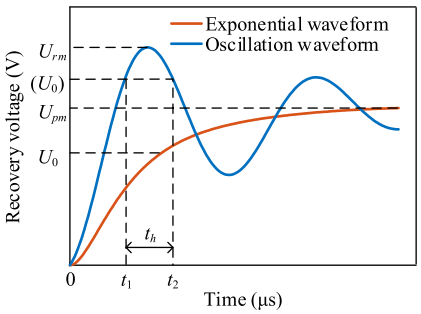

FIGURE 2. Schematic diagram of the recovery voltage waveform.

According to [25], there are two kinds of breakdowns: instantaneous reignition and delayed reignition. For the former, the arc reignites immediately after the current zero-crossing, while for the latter, the reignition takes place a specific period after the current zero-crossing. For an air circuit breaker with a low voltage level, it is mainly an instantaneous breakdown. That is, the breakdown occurs at the early stage of contact separation. At this time, the contact breaks instantly, and the metal on the contact surface melts and forms a liquid metal bridge. With increasing current density, metal vapor enters the contact gap. Then, under the external voltage, the gas molecules are heated, and the air is ionized. At the initial stage of contact separation, the temperature and particle concentration remain in a particular range. The external voltage intensity and contact gap play a dominant role in the reignition. In addition, the contact material also affects the reignition of the low-voltage circuit breaker. This paper mainly analyzes the same low-voltage circuit breakers, and the influence of contact materials on reignition can be considered fixed.

In Fig. 2, U_0 is the static breakdown voltage. If U_0 continually acts on the contact gap, gap breakdown occurs; U_{rm} is the peak recovery voltage; U_{pm} is the instantaneous value of the power supply voltage at both ends of the contact; t_h is the total time that the recovery voltage is higher than the gap breakdown voltage. For exponential recovery voltage, the circuit breaker reignition is only related to U_{pm} and U_0. When $U_{pm} < U_0$, the recovery voltage is always less than the contact gap dielectric strength. The arc is extinguished at the zero-crossing. When $U_{pm} > U_0$, the dielectric strength of the contact gap cannot withstand the action of the recovery voltage, which leads to circuit breaker reignition. Its probability is fixed at 1.

For a voltage waveform with oscillation characteristics, the recovery voltage is not always higher than the gap breakdown voltage. The discharge time lag (the time needed from electron generation to gap breakdown completion) of gap breakdown should be considered in analyzing the low-voltage circuit breaker reignition. When $U_{pm} < U_0 < U_{rm}$, if t_h is greater than the discharge time lag, the discharge conditions can be met. The form of gas discharge transitions from glow discharge to arc discharge. Then, gap breakdown is completed, and the circuit breaker ignites again. If t_h is less than the discharge time lag, the discharge process cannot be completed, the recovery voltage drops below U_0, and the arc is extinguished. The discharge time lag value is random. It usually follows a normal distribution, so the reignition probability is not 1 but varies with the contact gap and the recovery voltage.

When $U_{pm} > U_0$, the low-voltage circuit breaker reignition is similar to the previous reignition that appears in the exponential waveform, and the reignition probability is fixed at 1.

According to the air gap discharge characteristics [26], [27], there is a complex multidimensional nonlinear relationship between gap breakdown and various factors, such as the contact structure, voltage waveform, and atmospheric environment. However, when the voltage waveform and environmental features of the same gap remain unchanged, the breakdown voltage distribution remains in a particular range. During the interruption of the low-voltage circuit breaker, the contact gap itself changes. The breakdown voltage under these conditions depends on the contact gap, contact material, and current zero-crossing condition (current intensity, temperature). This paper assumes that the manufacturing errors and contact structure of the same batch of products can be ignored. When the running environment is constant, the contact gap breakdown voltage distribution is determined.

B. REIGNITION PROBABILITY MODEL BASED ON ASPA

Under different recovery voltages, the reignition probability model must first be established to analyze the reignition characteristics and their influence on the low-voltage circuit breaker electrical life under different running conditions. It is difficult to measure the contact gap of the low-voltage circuit breaker online. The information directly related to the low-voltage circuit breaker electrical life (such as arcing time) cannot be reflected through the contact gap. Therefore, it is necessary to use other characteristic parameters to describe the low-voltage circuit breaker reignition more concisely.

The ASPA is the current phase angle at the moment of arcing, which judges the circuit breaker breaking time. Its range is $[0, \pi]$. Depending on the ASPA, the contact gap is different at the zero-crossing current, and the breakdown voltage is also different. The larger the ASPA is, the smaller the contact gap is, and at the current zero-crossing, the smaller the breakdown voltage required for air breakdown is. It is assumed that the

recovery voltage is constant for the same type of low-voltage circuit breaker when the arc is extinguished. When ASPA is larger than a specific value, the breakdown voltage is less than the recovery voltage, and arc reignition occurs. Therefore, we can establish the corresponding relationship between the starting phase angle and the reignition.

The circuit breaker interruption meets two preconditions. First, there is a uniform electric field between the circuit breaker contacts, and the air medium meets the breakdown condition of Paschen's law [27]. Second, when the gap changes little, the breakdown voltage has a linear relationship with the gap distance [28]. According to the different recovery voltages, the low-voltage circuit breaker reignition can be divided into the following:

Case 1: the recovery voltage rises exponentially. There is a phase angle φ_1. When the ASPA is greater than φ_1, the low-voltage circuit breaker reignites, and the reignition probability is 1. When the ASPA is less than φ_1, the arc of the low-voltage circuit breaker is extinguished at the zero-crossing, and no reignition occurs. We call φ_1 the minimum reignition phase angle (MRPA).

Case 2: the recovery voltage oscillates. The peak recovery voltage is greater than the instantaneous value of the power supply voltage, which can theoretically be up to $2U_{pm}$. The breakdown gap is larger than in case 1. There are phase angles φ_1 and φ_2 ($\varphi_2 < \varphi_1$). If the ASPA is less than φ_2, the arc of the low-voltage circuit breaker is extinguished at the zero-crossing, and no reignition occurs. If the ASPA is greater than φ_1, the arc reignites, and the reignition probability is 1, which is the same as in case 1. If ASPA is in $[\varphi_2, \varphi_1]$, the reignition probability increases as ASPA increases. At present, the Weibull distribution is usually used for statistical analysis of breakdown voltage. When the interval between φ_2 and φ_1 is not large, the reignition probability increases approximately linearly with the ASPA [28]. We call φ_2 the critical reignition phase angle (CRPA).

To analyze the reignition rule of low-voltage circuit breakers under different conditions more intuitively, we calculate the reignition probability formula of single-pole contact and three-pole contact and draw the reignition probability change curve. The reignition probability of the single-pole contact is given in equations (1) and (2).

Case 1:

$$P_{\mathrm{F}} = \begin{cases} 1, & \varphi \in [\varphi_1, \pi) \\ 0, & \text{others} \end{cases} \tag{1}$$

Case 2:

$$P_{\mathrm{S}} = \begin{cases} 1, & \varphi \in [\varphi_1, \pi) \\ \dfrac{\varphi - \varphi_2}{\varphi_1 - \varphi_2}, & \varphi \in [\varphi_2, \varphi_1) \\ 0, & \text{others} \end{cases} \tag{2}$$

For well-designed low-voltage circuit breakers, the dielectric strength recovery speed should comply with the specified requirements and quickly ensure that the contact gap returns to the insulation state [29], [30]. Therefore, the MRPA and CRPA for single-pole and three-pole contacts are not too small. In this paper, taking φ_2 and $\varphi_1 \in (2\pi/3, \pi)$ as an example, the impact of reignition on electrical life is illustrated. The variation law of the reignition probability of single-pole contact with ASPA is shown in Fig. 3.

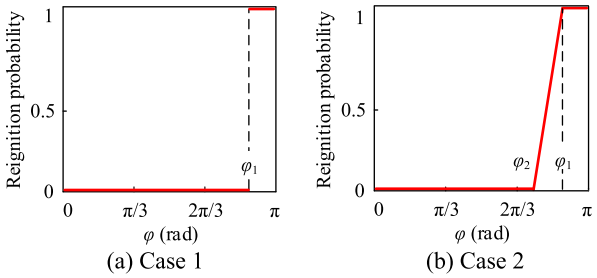

FIGURE 3. Reignition probability of single-pole contact.

For a three-phase circuit, we need to consider the role of the neutral line. The neutral line is a wire drawn from the neutral point N of a three-phase winding with a Y connection. When the neutral line exists (three-phase four-wire system), the load phase voltage is symmetrical and always equal to the power supply phase voltage. The purpose is to make each phase load independent of the others. When one phase is disconnected, the other two phases' load is not affected. If three-phase load balancing (such as the three-phase electric furnace and three-phase motor) occurs, the three-phase three-wire system can meet the power supply requirements, and no neutral line is needed at this time. The three-phase three-wire system is cost-saving and straightforward and is usually used in transmission and substation. The two connection modes need to be determined according to actual conditions. For the connection with neutral lines, one phase current of the three-phase circuit crosses zero, which does not affect the other two-phase circuit. For the connection with no neutral line, one phase current of the circuit is zero, and the other two-phase currents are changed.

The phase difference of the three-phase current is $2\pi/3$, and the reignition probability of the three-pole contact is different from that of the single-pole contact. The reignition of each phase interval of different ASPAs should be analyzed separately. When $\varphi_2, \varphi_1 \in (2\pi/3, \pi)$, the low-voltage circuit breaker has a single-phase reignition, and the three-pole contact reignition probability formulas are as follows:

Case 1:

$$P_{\mathrm{FA}} = \begin{cases} 1, & \varphi_{\mathrm{A}} \in [\varphi_1, \pi) \\ 0, & \text{others} \end{cases} \tag{3}$$

$$P_{\mathrm{FB}} = \begin{cases} 1, & \varphi_{\mathrm{A}} \in [\varphi_1 - \dfrac{\pi}{3}, \dfrac{2\pi}{3}) \\ 0, & \text{others} \end{cases} \tag{4}$$

$$P_{\mathrm{FC}} = \begin{cases} 1, & \varphi_{\mathrm{A}} \in [\varphi_1 - \dfrac{2\pi}{3}, \dfrac{\pi}{3}) \\ 0, & \text{others} \end{cases} \tag{5}$$

Case 2:

$$P_{SA}=\begin{cases}1, & \varphi_A\in[\varphi_1,\pi)\\ \dfrac{\varphi_A-\varphi_2}{\varphi_1-\varphi_2}, & \varphi_A\in[\varphi_2,\varphi_1)\\ 0, & \text{others}\end{cases}\tag{6}$$

$$P_{SB}=\begin{cases}1, & \varphi_A\in[\varphi_1-\dfrac{\pi}{3},\dfrac{2\pi}{3})\\ \dfrac{(\varphi_A+\pi/3)-\varphi_2}{\varphi_1-\varphi_2}, & \varphi_A\in[\varphi_2-\dfrac{\pi}{3},\varphi_1-\dfrac{\pi}{3})\\ 0, & \text{others}\end{cases}\tag{7}$$

$$P_{SC}=\begin{cases}1, & \varphi_A\in[\varphi_1-\dfrac{2\pi}{3},\dfrac{\pi}{3})\\ \dfrac{(\varphi_A+2\pi/3)-\varphi_2}{\varphi_1-\varphi_2}, & \varphi_A\in[\varphi_2-\dfrac{2\pi}{3},\varphi_1-\dfrac{2\pi}{3})\\ 0, & \text{others}\end{cases}\tag{8}$$

The variation law of the reignition probability of three-pole contact with ASPA is shown in Fig. 3. The reignition probability curve is divided into six intervals, which are marked X_1-X_6 and Y_1-Y_6. In X_2, X_4, and X_6, reignition occurs, and there is no reignition in X_1, X_3, and X_5. This is the same as in case 2.

III. ARC EROSION MODEL OF THE LOW-VOLTAGE CIRCUIT BREAKER WITH REIGNITION PROBABILITY

A. ARC EROSION MODEL OF SINGLE-POLE CONTACT

When the switch's contact is separated, an arc appears between the contacts. The arc energy effect on contact is instantaneous and concentrated, and material evaporation and splash erosion occur on the contact surface, which affects the contact performance. Arc erosion shortens the electrical life of the switchgear. The mass loss of contact caused by arc erosion has a specific corresponding relationship with operation times, current, charge, arc energy, i^2t, t [9], [31], [32]. In combination with the conclusion of [8], i^2t can more accurately describe the impact of arc erosion on contacts in switchgear with a higher number of operations. This paper mainly analyzes the macrodistribution characteristics of electrical life on a low-voltage circuit breaker after reignition. Additionally, the same contact type can withstand the same contact erosion amount (CEA) [7], [33]. Therefore, we selected i^2t as the basic formula for calculating arc erosion.

For single-pole contact, when the low-voltage circuit breaker is reignited or not, the circuit current changes with the ASPA, as shown in Fig. 5.

When there is no reignition, the CEA caused by the breaking arc can be calculated by equation (9):

$$q=\frac{\alpha I^2}{\omega}\left(\pi-\varphi+\frac{1}{2}\sin 2\varphi\right),\quad \varphi\in[0,\pi)\tag{9}$$

where q is the CEA without reignition; α is the erosion factor related to the contact material and structure of the low-voltage circuit breaker; I is the effective value of the load current; and ω is the angular frequency of the AC power supply.

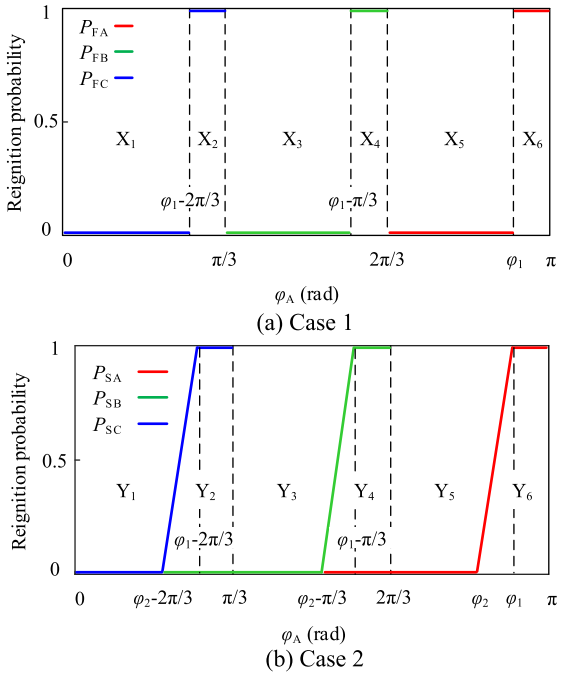

FIGURE 4. Reignition probability of three-pole contact.

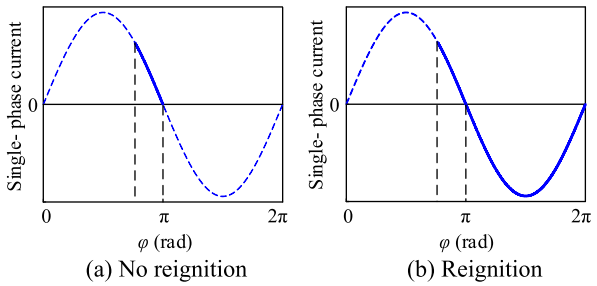

FIGURE 5. Circuit current variation law of single-pole contact.

Considering the influence of reignition on electrical life, the CEA can be calculated by equations (10) and (11):

$$q_F=\frac{\alpha I^2}{\omega}\left(\pi-\varphi+\frac{1}{2}\sin 2\varphi\right)+P_F\cdot\frac{\alpha\pi I^2}{\omega},\quad \varphi\in[0,\pi)\tag{10}$$

$$q_S=\frac{\alpha I^2}{\omega}\left(\pi-\varphi+\frac{1}{2}\sin 2\varphi\right)+P_S\cdot\frac{\alpha\pi I^2}{\omega},\quad \varphi\in[0,\pi)\tag{11}$$

where q_F and q_S are the CEAs for case 1 and case 2, respectively.

This paper describes the relationship between the CEA and the ASPA using the per-unit value of CEA $q/(\alpha I^2)$. The change law of $q/(\alpha I^2)$ with ASPA is shown in Fig. 6.

Fig. 6 shows that the CEA of the single-pole contact changes continuously and decreases with increasing ASPA when there is no reignition. In case 1, the CEA is discontinuous at φ_1, the maximum CEA appears in the interval $[\varphi_1,\pi]$, and there is the same CEA in other intervals compared with no reignition. In case 2, the CEA increases linearly in $[\varphi_2,\varphi_2]$,

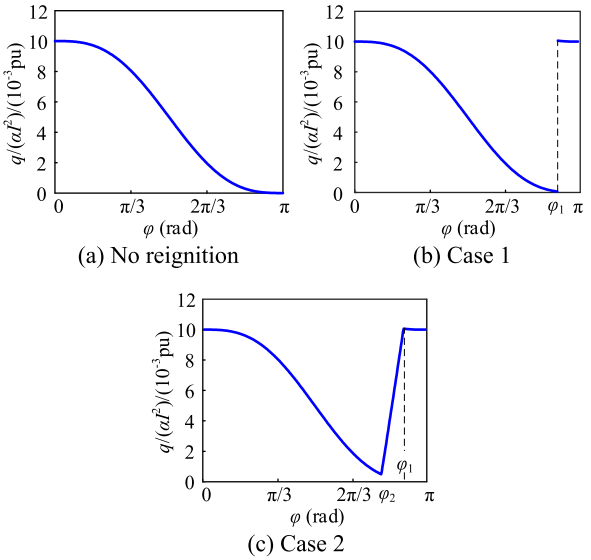

(a) No reignition (b) Case 1

(c) Case 2

FIGURE 6. Variation law of $q/(\alpha I^2)$ of single-pole contact.

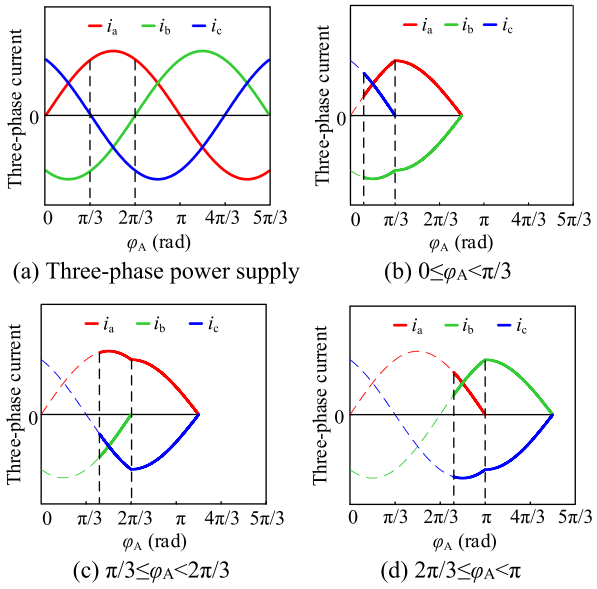

(a) Three-phase power supply (b) $0 \le \varphi_A < \pi/3$

(c) $\pi/3 \le \varphi_A < 2\pi/3$ (d) $2\pi/3 \le \varphi_A < \pi$

FIGURE 7. Circuit current variation law of three-pole contact.

the minimum CEA appears at φ_2, and there is the same CEA in other intervals compared with case 1.

B. ARC EROSION MODEL OF THREE-POLE CONTACT

In the three-phase power supply, when the neutral point of the three-phase load is connected with the neutral point of the power supply, each phase circuit's arcing time is the same as the case of the single-pole contact. The CEA can be calculated according to the condition of the single-pole contact. The electrical life of the low-voltage circuit breaker is determined by the contact with the most severe arc erosion. When there is no connection between the power supply and the three-phase load, the circuit topology changes once the arc of one phase extinguishes. The order of arc extinction should be considered when calculating the CEA. This paper mainly discusses the CEA of a three-pole contact when there is no connection between the power supply and the three-phase load. When the arc is normally extinguished, the variation law of the three-pole contact current with the ASPA is shown in Fig. 7 [8].

According to the current zero-crossing, the ASPA of the three-pole contact is divided into three intervals with $\pi/3$. In Fig. 7(b)-7(d), the two vertical dotted lines represent the arc starting time and arc extinguishing time of the first phase going through the current zero-crossing. The current dotted line represents the change in the current waveform when the contacts are not disconnected.

It is assumed that the second current zero-crossing phase does not reignite. The first arc-starting phase and each phase's arcing time changes after reignition. The variation law of the first arc-starting phase and the arcing time is shown in Table 1.

Taking φ_1 and $\varphi_2 \in [2\pi/3, \pi)$ as an example, the three-phase current varies with ASPA, as shown in Fig. 8.

When the arcing time changes, the current also changes. For example, the phase A arc is extinguished first when there is no reignition in $(2\pi/3, \pi)$, the effective value of the phase B and C currents change to $I\sqrt{3/2}$, and then the phase B and C arcs extinguish simultaneously.

When there is reignition, phase A's arcing time increases, and the effective value of the phase A current is I before the zero crossings of the phase C current. The effective value of the phase A current changes to $I\sqrt{3/2}$ after the phase C arc is extinguished. Phase B and C currents change similarly, so they should be considered to calculate arc erosion.

When there is no reignition, a specific phase of the three-pole contact extinguishes first, and then the other two phases extinguish at the same time after T/4. The CEA of phase A can be obtained by equation (12).

$$q_A = \begin{cases} \dfrac{\alpha I^2}{\omega}\left(\dfrac{\pi}{3} - \varphi_A + \dfrac{1}{2}\sin 2\varphi_A - \dfrac{\sqrt{3}}{4} + \dfrac{3\pi}{8}\right), \\ \qquad \varphi_A \in [0, \pi/3) \\ \dfrac{\alpha I^2}{\omega}\left(\dfrac{2\pi}{3} - \varphi_A + \dfrac{1}{2}\sin 2\varphi_A + \dfrac{\sqrt{3}}{4} + \dfrac{3\pi}{8}\right), \\ \qquad \varphi_A \in [\pi/3, 2\pi/3) \\ \dfrac{\alpha I^2}{\omega}\left(\pi - \varphi_A + \dfrac{1}{2}\sin 2\varphi_A\right), \\ \qquad \varphi_A \in [2\pi/3, \pi) \end{cases} \quad (12)$$

The CEA of phase A in $[0, \pi/3)$ is recorded as q_{A1} when there is no reignition. Similarly, they are defined as q_{A2} and q_{A3} in $[\pi/3, 2\pi/3)$ and $[2\pi/3, \pi)$.

To compare the difference and relationship of the CEA more intuitively, when reignition occurs or not, the CEA is expressed by q_{Ak} $(k = 1, 2, 3)$, which has the same calculation value as equation (12).

Fig. 4 shows that $[0, \pi]$ can be divided into six intervals, X_1-X_6 and Y_1-Y_6, according to the different reignition types. When calculating the CEAs, each phase's change in reignition probability in different intervals should be considered.

TABLE 1. Variation in the first arc-starting phase and the arcing time.

φ_A	First extinguishing-phase	Arcing time
$0\leq\varphi_A<\pi/3$	B	A phase +T/6
		B phase -T/12
		C phase +5T/12
$\pi/3\leq\varphi_A<2\pi/3$	A	A phase -T/12
		B phase +5T/12
		C phase +T/6
$2\pi/3\leq\varphi_A<\pi$	C	A phase +5T/12
		B phase +T/6
		C phase -T/12

"+" means the arcing time increases, "-" means the arcing time decreases, and T is the period of the power-frequency current.

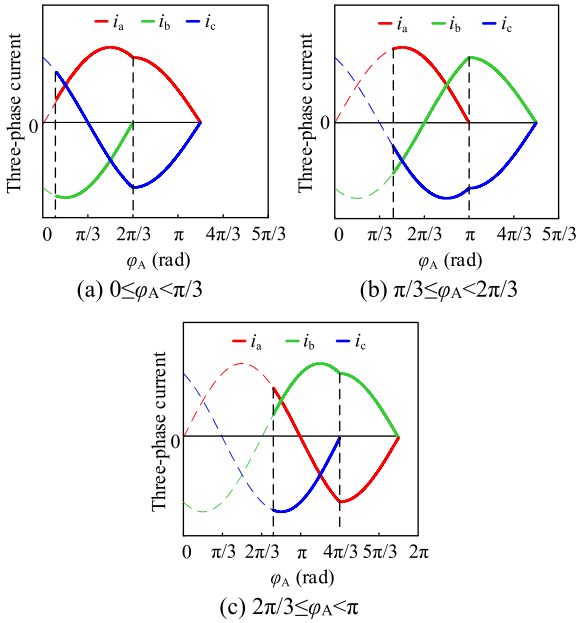

FIGURE 8. Circuit current variation law of three-pole contact with reignition.

In case 1 and case 2, the CEA of phase A can be calculated by equations (13) and (14):

Case 1:

$$q_{FA}=\begin{cases} q_{A1}+\dfrac{\alpha I^2}{\omega}\cdot P_{FC}\left(\dfrac{\pi}{3}+\dfrac{\sqrt{3}}{2}\right), \\ \qquad \varphi_A\in[0,\pi/3) \\ q_{A2}+\dfrac{\alpha I^2}{\omega}\cdot P_{FB}\left(\dfrac{\pi}{3}-\dfrac{\sqrt{3}}{4}-\dfrac{3\pi}{8}\right), \\ \qquad \varphi_A\in[\pi/3,2\pi/3) \\ q_{A3}+\dfrac{\alpha I^2}{\omega}\cdot P_{FA}\left(\dfrac{\pi}{3}-\dfrac{\sqrt{3}}{4}+\dfrac{3\pi}{8}\right), \\ \qquad \varphi_A\in[2\pi/3,\pi) \end{cases} \tag{13}$$

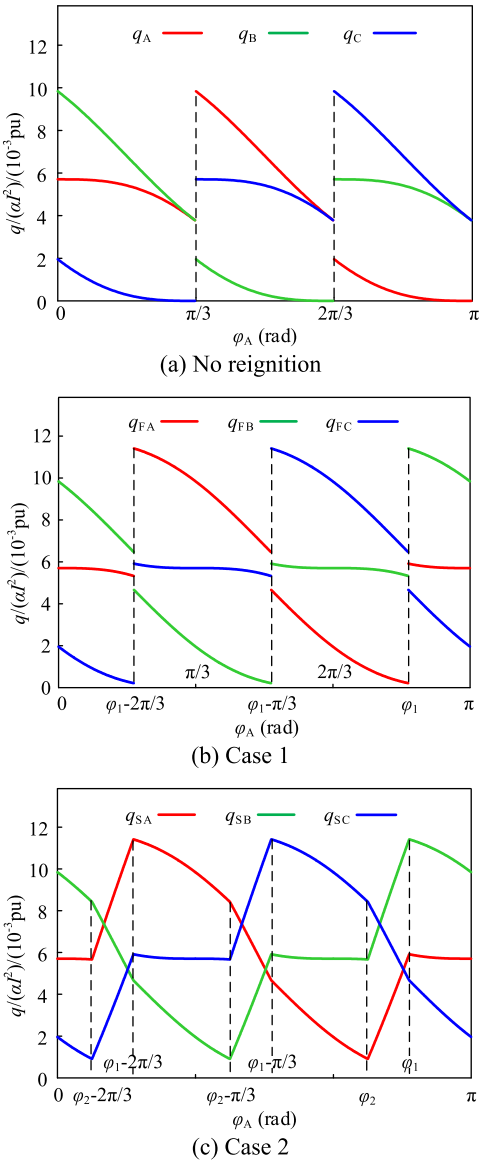

FIGURE 9. Variation law of $q/(\alpha I^2)$ of three-pole contact.

Case 2:

$$q_{SA}=\begin{cases} q_{A1}+\dfrac{\alpha I^2}{\omega}\cdot P_{SC}\left(\dfrac{\pi}{3}+\dfrac{\sqrt{3}}{2}\right), \\ \qquad \varphi_A\in[0,\pi/3) \\ q_{A2}+\dfrac{\alpha I^2}{\omega}\cdot P_{SB}\left(\dfrac{\pi}{3}-\dfrac{\sqrt{3}}{4}-\dfrac{3\pi}{8}\right), \\ \qquad \varphi_A\in[\pi/3,2\pi/3) \\ q_{A3}+\dfrac{\alpha I^2}{\omega}\cdot P_{SA}\left(\dfrac{\pi}{3}-\dfrac{\sqrt{3}}{4}+\dfrac{3\pi}{8}\right), \\ \qquad \varphi_A\in[2\pi/3,\pi) \end{cases} \tag{14}$$

According to the mathematical model of CEA of the three-pole contact under different reignition types, the change law of $q/(\alpha I^2)$ with the ASPA for three-pole contact is shown in Fig. 9.

Derived by equation (13), there is the same calculation equation in intervals X_2 and X_3 and the same as in X_4 and X_5. Therefore, the CEA curve of the three-pole contact is divided into four parts, as shown in Fig. 9 (b). In case 2, the CEA curve changes continuously and can be divided into six parts, as shown in Fig. 9 (c), and the CEA is the same as that without reignition in Y_1, Y_3, and Y_5. In addition, in both cases, the CEA's maximum value is greater than that of the CEA without reignition. Therefore, the influence of reignition on the electrical life of a low-voltage circuit breaker cannot be ignored.

When the current level is low, the arc erosion of the contact material is mainly related to the current size, duration, and contact material. When the current level is larger (more than 1 kA), contact repulsion, gas material, and arc motion also affect contact erosion. The arc temperature and magnetic force on the arc increase under high current conditions, the sudden change in the arc erosion rate, and the influence of the arc shape on the contact should be considered. This paper studies the electrical life of a low-voltage circuit breaker, and the erosion mechanism does not change under the default low current level.

IV. ELECTRICAL LIFE SIMULATION AND EXPERIMENT OF THE LOW-VOLTAGE CIRCUIT BREAKER

To further analyze the differences in the electrical life distribution of low-voltage circuit breakers under different reignition types, we also need to perform electrical life simulations. Based on the analysis of the change law of the CEA of a single-pole contact and three-pole contact, using the Monte Carlo method, we simulate the low-voltage circuit breaker electrical life test under random ASPA. This paper takes case 1 as an example. The simulation process is shown in Fig. 10.

The simulation steps are as follows:

1) The CEA threshold of the low-voltage circuit breaker is set;

2) The random ASPA is generated;

3) It is determined whether reignition occurs according to the reignition probability model and the values of φ_1 and φ_2;

4) The CEA of the single-phase (or three-phase) contact is calculated based on the result of 3);

5) The accumulative CEA Q_k ($k = 1, 2, 3$) of the single-phase (or three-phase) contact is calculated. If the minimum value of Q_k is greater than the CEA threshold, the life ends; otherwise, steps 2)-4) are repeated;

6) Steps 2)-5) are cycled n times independently and the n low-voltage circuit breakers' electrical life distribution is obtained.

In this paper, the load current and erosion factor are constant. The CEA threshold Q is replaced by the per-unit value Q^*. The average electrical life of the low-voltage circuit breaker can reach 10000 times. Equation (9) is integrated to obtain a single time average CEA, which is $\bar{q}$, $\bar{q} = \alpha I^2(5 \times 10^{-3})$, $Q^* = 10000 \times \bar{q}/\alpha I^2 = 50$. The test sample number is n, and its value is 1000.

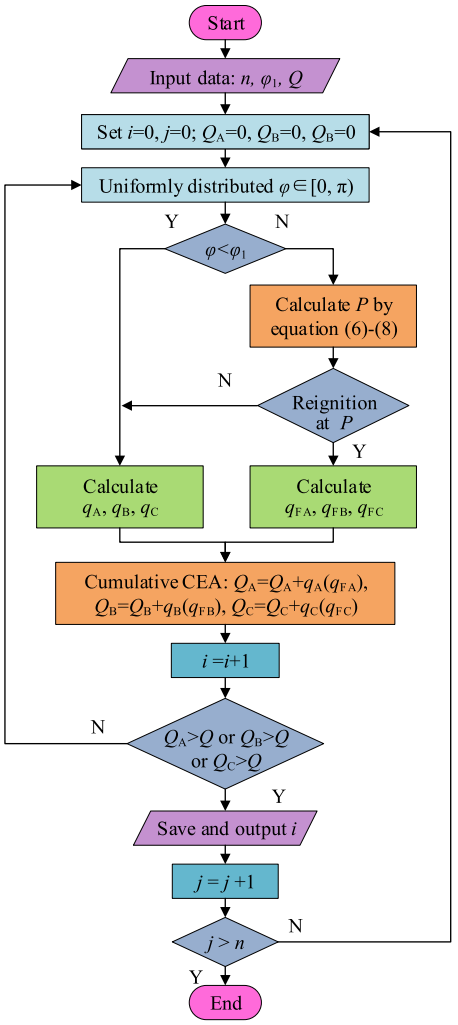

FIGURE 10. Flowchart of the electrical life simulation program.

A. SIMULATION TEST RESULT ANALYSIS OF THE SINGLE-PHASE CONTACT

The failure distribution function can reflect the product's failure law as a whole, and the life distribution of the product can be characterized with life as a random variable. Common life distribution types include the exponential distribution, Weibull distribution, lognormal distribution, and normal distribution [34]–[37]. For switching appliances, there are normal distributions and Weibull distributions [8]. Using statistical methods to perform hypothesis testing and parameter estimation on the distribution function, we can understand the products' life characteristics more intuitively. The relevant statistical parameters have two other uses: planning maintenance strategies for electrical products and collecting basic information in life cycle management. In this paper, the electrical life of a single-pole contact is simulated. The frequency distribution histograms of electrical life are obtained under the different reignition types, as shown in Fig. 11. The values of φ_1 and φ_2 are 0.85π and 0.75π, respectively.

It can be observed in Fig. 11 that the electrical life distribution of a single-pole contact is approximately normally

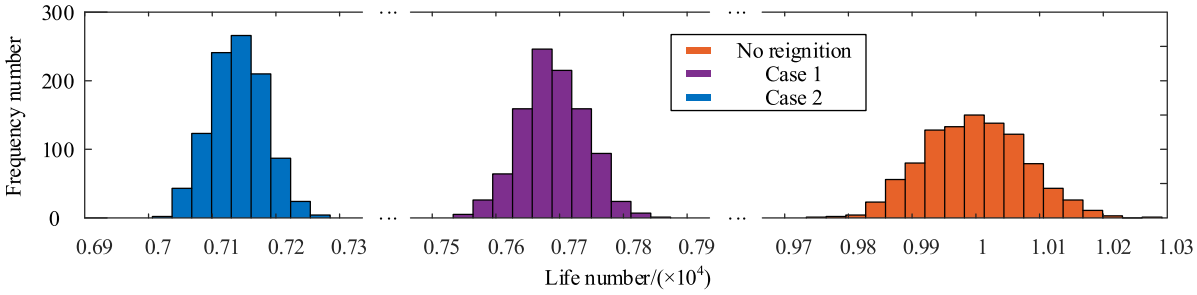

FIGURE 11. Histogram of electrical life of single-pole contact.

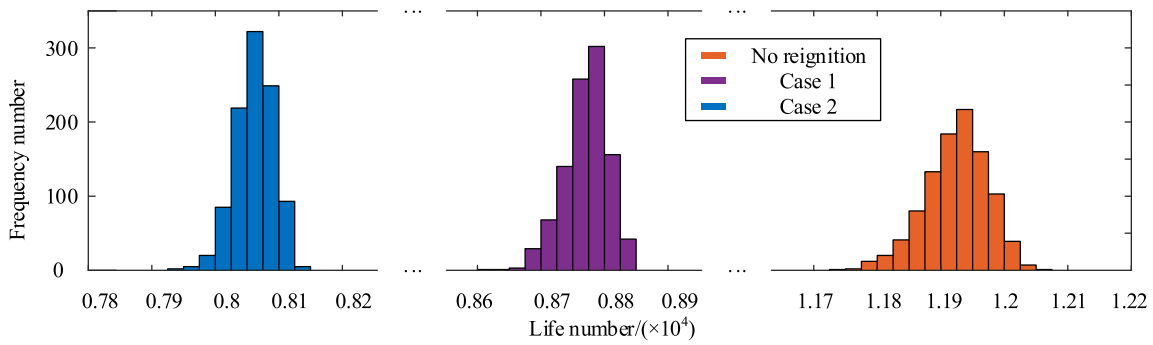

FIGURE 12. Histogram of electrical life of three-pole contact.

TABLE 2. Statistics of electrical life of single-pole contact.

Statistics	No reignition	Case 1	Case 2
μ	9997	7690	7141
σ	79	50	42
Max	10266	7844	7271
Min	9761	7549	7013

μ is the mean of the normal distribution; σ is the standard deviation; Max and Min are the maximum and minimum life of the single-pole contact, respectively.

TABLE 3. Statistics of electrical life of three-pole contact.

Statistics	No reignition	Case 1	Case 2
m	7	9	7
t	299	263	206
v	11645	8522	7867
Max	12051	8845	8146
Min	11732	8620	7935
μ_w	11925	8771	8061
σ_w	47	33	30

m is the shape parameter, t is the scale parameter, v is the position parameter, μ_w is the mean value of the Weibull distribution, and σ_w is the standard deviation of the Weibull distribution.

distributed under different reignition types. The normal distribution test with a significance level of p =0.05 was used, and each parameter's statistical values are given in Table 2.

From Table 2, the average electrical life of a single-pole contact after considering reignition is significantly shorter than that without reignition. Furthermore, by comparing σ under different reignition types, the dispersion of the electrical life changes when there is reignition, decreasing with reignition times.

B. SIMULATION TEST RESULT ANALYSIS OF THE THREE-PHASE CONTACT

The electrical life of the three-pole contact is simulated, and φ_1 and φ_2 are taken as 0.85π and 0.75π, respectively. The frequency distribution histograms of the electrical life are shown in Fig. 12.

According to Fig. 12, the electrical life distribution of the three-pole contact is approximately a Weibull distribution under different reignition types. The significant level p =0.05 Weibull distribution test is carried out. The statistical values of each parameter are given in Table 3.

This paper analyzes the statistical data in Table 3 and Table 4. For the single-pole contact, the low-voltage circuit breaker average electrical life is 76.9% and 71.4% of that without reignition in case 1 and case 2, respectively. For the three-pole contact, they are 73.6% and 67.6%, respectively. The electrical life of the low-voltage circuit breaker is reduced after reignition, and case 2 is more severe than case 1. Meanwhile, the effect of reignition under the single-pole contact condition is more significant than that under the three-pole contact condition. Therefore, the distribution of the low-voltage circuit breaker electrical life should be judged according to different reignition types.

φ_1 and φ_2 are not fixed in real life, and the reignition probability can be evaluated by calculating the grid and load parameters and testing the circuit breaker. We should

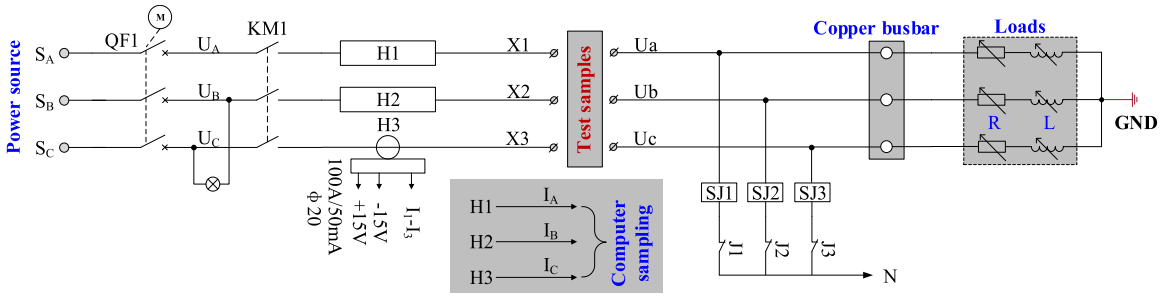

FIGURE 13. Main circuit diagram of the circuit breaker electrical operation reliability test device.

TABLE 4. Configuration parameters of test platform.

Parameters	Value
Type of circuit breaker	DZ47-63
Rated current I_e/A	20
Rated voltage U_e/V	220
Test current I/I_e	1
Test voltage U/U_e	1
Voltage on the coil/V	380
Electricity frequency/Hz	50
Power factor	0.35-0.95
Operation frequency (Times/h)	120

judge the electrical life distribution according to the running conditions.

C. ELECTRICAL LIFE TEST OF THE LOW-VOLTAGE CIRCUIT BREAKER

This paper adds relevant electrical life experiments to prove the reignition of a low-voltage circuit breaker under different running conditions. Different power factors (0.35-0.95) were selected to conduct several breaking tests and count the low-voltage circuit breaker reignition condition. The main circuit diagram of the breaking operation test is illustrated in Fig. 13. QF1 is the circuit breaker with shunt tripping used to protect and control the entire test device. KM1 is an auxiliary test contactor that can connect the power supply. H1∼H3 are Hall sensors used for the current signal collection. SJ1∼SJ3 are time relays, which can be used as hardware protection for fault removal and alarm reminders. X1∼X3 and U_a ∼U_c are voltage sampling points. The experimental parameters are shown in Table 4. The test equipment is illustrated in Fig. 14.

According to the test parameters in Table 4, the air circuit breaker electrical life test with loads is carried out. The number of breaking operations under each power factor is 200. The sampling frequency for the current is 2 K/s, and for the voltage it is 1 K/s, and the arc reignition waveform is shown in Fig. 15. Z_1 ∼Z_3 are the arc starting time, arc reignition time, and three-phase arc extinguishing time, respectively. u_c is the arc voltage of phase C.

The statistical MRPA and q^* under different power factors are given in Table 5. q^* is the calculated average CEA where

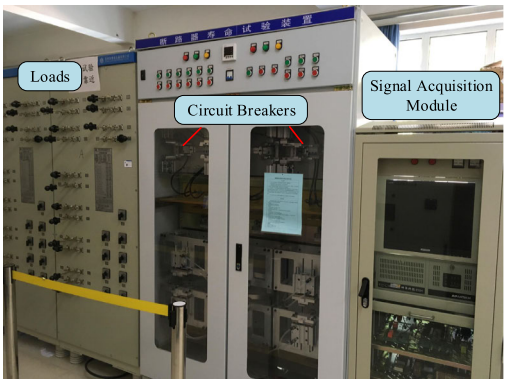

FIGURE 14. Experimental platform.

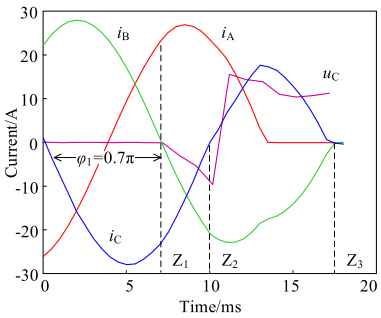

FIGURE 15. The current waveform with reignition.

TABLE 5. The MRPA under different power factors.

Power factor	φ_1	q^*/A^2·s
0.35	0.7π	2.75
0.45	0.75π	2.53
0.65	0.85π	2.12
0.75	0.9π	1.94
0.95	No reignition	1.11

the ASPA is from 0 to π. According to the statistics, the reignition is the same as that in case 1. The power factor during the test is changed by adjusting the load, and the reignition condition is counted. With the increase in the power factor, the MRPA increases gradually. When the power factor is 0.95, no reignition occurs.

TABLE 6. The electrical life ratio under different power factors.

N/N_0	Power factor				
	0.35	0.45	0.65	0.75	0.95
Test	60.7%	66%	78.8%	86.1%	118%
Simulation	58.2%	62.5%	73.6%	80.7%	1

The relative remaining life of the low-voltage circuit breaker contacts can be expressed by equation (15) [8].

$$L = L_{\text{int}} - \sum_{j=1}^{N} \frac{q_j}{Q} \leq 0 \tag{15}$$

where L_{int} is the initial value of contact relative electrical life, $L_{\text{int}} \in [0, 1]$. For brand new products, $L_{\text{int}} = 1$.

When the contact fails, the remaining relative electrical life is 0. The relationship between q^* and life number N is shown as equation (16).

$$L_{\text{int}} = \sum_{j=1}^{N} \frac{q_j}{Q} = \frac{q^* \cdot N}{Q} = 1 \tag{16}$$

According to equation (16), for a low-voltage circuit breaker contact with a certain threshold Q, q^* is inversely proportional to N when the contact fails. Taking the contact life without reignition (defined as N_0) as the benchmark, the electrical life ratio under different power factors is shown in Table 6. It shows that the reignition probability is different, and the electrical life is different under different loads. Due to the current limiting effect of the low-voltage circuit breaker, the actual electrical life is slightly longer than the simulated life, but the life variation trend is consistent.

This paper studies the relationship between arc reignition and the electrical life of a low-voltage circuit breaker. According to the research results, it is possible to reduce the arc reignition impact on contact erosion by adjusting the load conditions and adding an overvoltage suppression module without changing the line efficiency. In addition, we can improve the electrical life by optimizing the contact structure (double-break structure) or intelligent breaking (controlling the ASPA distribution range).

V. CONCLUSION

Based on erosion characteristics of arc current on single-pole contact and three-pole contact under different reignition types, a low-voltage circuit breaker arc erosion model with reignition is established. This model can reflect the variation law of electrical life on low-voltage circuit breakers more accurately under various running conditions. Simultaneously, combining this model with the Monte Carlo method, the electrical life distribution of single-pole and three-pole contacts is simulated. It can help people evaluate the life distribution characteristics of low-voltage circuit breakers more effectively. The electrical life test of the air circuit breaker shows that under different load conditions, the MRPA is different. The probability of reignition is different, which corroborates the validity of the reignition probability model. Future work can start by reducing reignition and improving the electrical life of low-voltage circuit breakers.

REFERENCES

[1] L. Kui, L. Jian-Guo, W. Yi, Q. Zhi-Jun, and Y. Dong-Mei, "Research on the overload protection reliability of moulded case circuit-breakers and its test device," *J. Zhejiang Univ., Sci. A, Int. Appl. Phys. Eng. J.*, vol. 3, pp. 121–126, Mar. 2007.

[2] J. I. Melecio and H. Ahuett-Garza, "Design, analysis, and testing of a new microcircuit breaker thermal trip unit concept based on compliant mechanisms," *IEEE Trans. Ind. Appl.*, vol. 51, no. 4, pp. 2862–2873, Jul. 2015.

[3] A. A. Razi-Kazemi, "Applicability of auxiliary contacts in circuit breaker online condition assessment," *Electr. Power Syst. Res.*, vol. 128, pp. 53–59, Nov. 2015.

[4] Z. Fu, W. Chen, Z. Li, L. Xiang, C. Li, K. Bian, L. Wang, and B. Liu, "Wear mechanism and mass loss characteristic of arcing contacts in SF_6 circuit breaker in making process," *IEEE Trans. Compon., Packag., Manuf. Technol.*, vol. 8, no. 9, pp. 1593–1603, Sep. 2018.

[5] M. Mohammadhosein, K. Niayesh, A. A. Shayegani-Akmal, and H. Mohseni, "Online assessment of contact erosion in high voltage gas circuit breakers based on different physical quantities," *IEEE Trans. Power Del.*, vol. 34, no. 2, pp. 580–587, Apr. 2019.

[6] Z. Wu, G. Wu, H. Huang, and Y. You, "A novel residual electrical endurance prediction method for low-voltage electromagnetic alternating current contactors," *IEEE Trans. Compon., Packag., Manuf. Technol.*, vol. 5, no. 4, pp. 465–473, Apr. 2015.

[7] C. Zhiyuan, M. Shaohua, L. Wei, W. Jian, and W. Erzhi, "Monitor of electrical endurance of vacuum circuit breaker's contacts," in *Proc. 20th Int. Symp. Discharges Electr. Insul. Vac.*, 2002, pp. 483–486.

[8] S. Zheng, F. Niu, K. Li, S. Huang, Z. Liu, and Y. Wu, "Analysis of electrical life distribution characteristics of AC contactor based on performance degradation," *IEEE Trans. Compon., Packag., Manuf. Technol.*, vol. 8, no. 9, pp. 1604–1613, Sep. 2018.

[9] K. Li, C. Zhao, F. Niu, S. Zheng, Y. Duan, S. Huang, and Y. Wu, "Electrical performance degradation model and residual electrical life prediction for AC contactor," *IEEE Trans. Compon., Packag., Manuf. Technol.*, vol. 10, no. 3, pp. 400–417, Mar. 2020.

[10] W. Li, K. Li, L. Sun, S. Zhao, and L. Ji, "The test data verifying & prediction model of electrical contact," in *Proc. 50th IEEE Holm Conf. Electr. Contacts, 22nd Int. Conf. Electr. Contacts Electr. Contacts*, Sep. 2004, pp. 429–436.

[11] Z. Li, D. Jiang, W. Li, X. Su, and H. Guo, "Reliability analysis and failure prediction study of dynamic contact resistance on contact," in *Proc. IEEE Holm Conf. Electr. Contacts*, Oct. 2002, pp. 61–65.

[12] P. Dehghanian, Y. Guan, and M. Kezunovic, "Real-time life-cycle assessment of high-voltage circuit breakers for maintenance using online condition monitoring data," *IEEE Trans. Ind. Appl.*, vol. 55, no. 2, pp. 1135–1146, Apr. 2019.

[13] A. Bagherpoor, S. Rahimi-Pordanjani, A. A. Razi-Kazemi, and K. Niayesh, "Online condition assessment of interruption chamber of gas circuit breakers using arc voltage measurement," *IEEE Trans. Power Del.*, vol. 32, no. 4, pp. 1776–1783, Aug. 2017.

[14] Z. Wu, G. Wu, M. Dapino, L. Pan, and K. Ni, "Model for variable-length electrical arc plasmas under AC conditions," *IEEE Trans. Plasma Sci.*, vol. 43, no. 8, pp. 2730–2737, Aug. 2015.

[15] A. Iturregi, B. Barbu, E. Torres, F. Berger, and I. Zamora, "Electric arc in low-voltage circuit breakers: Experiments and simulation," *IEEE Trans. Plasma Sci.*, vol. 45, no. 1, pp. 113–120, Jan. 2017.

[16] Q. Wu, G. Xu, M. Yuan, and C. Wu, "Influence of operation numbers on arc erosion of Ag/CdO electrical contact materials," *IEEE Trans. Compon., Packag., Manuf. Technol.*, vol. 10, no. 5, pp. 845–857, May 2020.

[17] C. Ding, C. Li, Z. Yuan, and C. Fang, "An estimation method of Cu-W arcing contact electrical life of SF_6 circuit breakers in making capacitor bank," in *Proc. IEEE Holm Conf. Electr. Contacts*, Sep. 2019, pp. 101–107.

[18] B. Feizifar and O. Usta, "A novel arcing power-based algorithm for condition monitoring of electrical wear of circuit breaker contacts," *IEEE Trans. Power Del.*, vol. 34, no. 3, pp. 1060–1068, Jun. 2019.

[19] J. Tepper, M. Seeger, T. Votteler, V. Behrens, and T. Honig, "Investigation on erosion of Cu/W contacts in high-voltage circuit breakers," *IEEE Trans. Compon. Packag. Technol.*, vol. 29, no. 3, pp. 658–665, Sep. 2006.

[20] "Electrical breakdown voltage in micro- and submicrometer contact gaps (100 nm-10 m) in air and nitrogen," in *Proc. IEEE 61st Holm Conf. Elect. Contacts (Holm)*, San Diego, CA, USA, Oct. 2015.
[21] D. Shin, I. O. Golosnoy, and J. W. McBride, "Experimental study of reignition evaluators in low-voltage switching devices," *IEEE Trans. Compon., Packag., Manuf. Technol.*, vol. 8, no. 6, pp. 950–957, Jun. 2018.
[22] W. Hauer and Z. Xin, "Re-ignition and post arc current phenomena in low voltage circuit breaker," in *Proc. Int. Conf. Elect. Contacts (ICEC)*, 2014, pp. 1–6.
[23] E. Dullni, W. Shang, D. Gentsch, I. Kleberg, and K. Niayesh, "Switching of capacitive currents and the correlation of restrike and pre-ignition behavior," *IEEE Trans. Dielectr. Electr. Insul.*, vol. 13, no. 1, pp. 65–71, Feb. 2006.
[24] H. Liu, R. Li, D. He, J. Wei, and Q. Li, "Experimental study of multiple-reignition features of secondary arcs on EHV/UHV transmission lines," *IEEE Trans. Ind. Electron.*, vol. 66, no. 4, pp. 3247–3255, Apr. 2019.
[25] S. M. Wong, "Overvoltages and reignition behavior of vacuum circuit breaker," in *Proc. 6th Int. Conf. Adv. Power Syst. Control, Oper. Manage. (APSCOM)*, 2003, pp. 653–658.
[26] G. Galli, H. Hamrita, C. Jammes, M. J. Kirkpatrick, E. Odic, P. Dessante, and P. Molinié, "Paschen's law in extreme pressure and temperature conditions," *IEEE Trans. Plasma Sci.*, vol. 47, no. 3, pp. 1641–1647, Mar. 2019.
[27] D. B. Go and D. A. Pohlman, "A mathematical model of the modified Paschen's curve for breakdown in microscale gaps," *J. Appl. Phys.*, vol. 107, no. 10, pp. 231–269, 2010.
[28] R. Arora and W. Mosch, *High Voltage and Electrical Insulation Engineering* (Arora/High Voltage and Electrical Insulation). Hoboken, NJ, USA: Wiley, 2011, pp. 319–370.
[29] Y. M. Cho, J. H. Rhee, J. E. Baek, and K. C. Ko, "Implementing a dielectric recovery strength measuring system for molded case circuit breakers," *J. Electr. Eng. Technol.*, vol. 13, no. 4, pp. 1–7, 2018.
[30] K.-A. Lee and K.-C. Ko, "Experimental investigation of improvement in the dielectric recovery characteristics of a molded case circuit breaker splitter plate," *J. Electr. Eng. Technol.*, vol. 15, no. 2, pp. 757–763, Mar. 2020.
[31] J. J. Shea, "Erosion and resistance characteristics of AgW and AgC contacts," *IEEE Trans. Compon. Packag. Technol.*, vol. 22, no. 2, pp. 331–336, Jun. 1999.
[32] J. J. Shea, "High current AC break arc contact erosion," in *Proc. IEEE Holm Conf. Electr. Contacts*, Oct. 2008, pp. 23–46.
[33] M. T. Dhotre, X. Ye, and S. Kotilainen, "Contact erosion in high voltage circuit breakers," in *Proc. IEEE Electr. Insul. Conf. (EIC)*, Jun. 2018, pp. 448–451.
[34] S. R. Cain, "Distinguishing between lognormal and Weibull distributions," *IEEE Trans. Rel.*, vol. 51, no. 1, pp. 32–38, Mar. 2002.
[35] D. H. Collins and R. L. Warr, "Failure time distributions for complex equipment," *Qual. Rel. Eng. Int.*, vol. 35, no. 1, pp. 146–154, Feb. 2019.
[36] J. Fan, C. Qian, K.-C. Yung, X. Fan, G. Zhang, and M. Pecht, "Optimal design of life testing for high-brightness white LEDs using the six sigma DMAIC approach," *IEEE Trans. Device Mater. Rel.*, vol. 15, no. 4, pp. 576–587, Dec. 2015.
[37] Y. Yang and F. Guo, "Reliability analysis of aero-equipment components life based on normal distribution model," in *Proc. IEEE 4th Inf. Technol. Mechatronics Eng. Conf. (ITOEC)*, Dec. 2018, pp. 1070–1074.

ZHENGJUN LIU (Graduate Student Member, IEEE) was born in China, in 1989. He received the B.S. degree in mechatronic engineering from Jiangsu University, Zhenjiang, China, in 2013, and the M.S. degree in mechatronic engineering from Dalian Jiaotong University, Dalian, China, in 2016. He is currently pursuing the Ph.D. degree in electrical engineering with the Hebei University of Technology, Tianjin, China.

His current research interest includes electrical equipment reliability theory and application.

SHAOPO HUANG was born in Xingtai, China, in 1986. He received the B.S. and M.S. degrees in electrical engineering from the Hebei University of Technology, Tianjin, China, in 2009 and 2012, respectively, where he is currently pursuing the Ph.D. degree in electrical engineering.

From 2017 to 2019, he was a Research Fellow with the Electrical Machines and Drives Laboratory, Michigan State University, East Lansing, MI, USA. His current research interests include reliability and life prediction of electrical apparatus and fault.

CHENGCHEN ZHAO was born in Zhangjiakou, China, in 1991. She received the B.S. degree in electronic information science and technology and the M.S. degree in communication and information systems from Hebei University, Baoding, China, in 2014 and 2017, respectively. She is currently pursuing the Ph.D. degree in electrical engineering with the Hebei University of Technology, Tianjin, China.

Her current research interests include reliability and life prediction of electrical apparatus.